

# Coupling an HCN2-expressing cell to a myocyte creates a two-cell pacing unit

V. Valiunas<sup>1</sup>, G. Kanaporis<sup>1</sup>, L. Valiuniene<sup>1</sup>, C. Gordon<sup>1</sup>, H. Z. Wang<sup>1</sup>, L. Li<sup>1</sup>, R. B. Robinson<sup>2</sup>, M. R. Rosen<sup>2</sup>, I. S. Cohen<sup>1</sup> and P. R. Brink<sup>1</sup>

<sup>1</sup>Department of Physiology and Biophysics and the Institute for Molecular Cardiology, State University of New York at Stony Brook, Stony Brook, NY, USA

<sup>2</sup>Department of Pharmacology and the Center for Molecular Therapeutics, Columbia University, New York, NY, USA

We examined whether coupling of a ventricular myocyte to a non-myocyte cell expressing HCN2 could create a two-cell syncytium capable of generating sustained pacing. Three non-myocyte cell types were transfected with the mHCN2 gene and used as sources of mHCN2-induced currents. They were human mesenchymal stem cells and HEK293 cells, both of which express connexin43 (Cx43), and HeLa cells transfected with Cx43. Cell–cell coupling between heterologous pairs increased with time in co-culture, and hyperpolarization of the myocyte induced HCN2 currents, indicating current transfer from the mHCN2-expressing cell to the myocyte via gap junctions. The magnitude of the HCN2 currents recorded in myocytes increased with increasing junctional conductance. Once a critical level of electrical cell–cell coupling between myocytes and mHCN2 transfected cells was exceeded spontaneous action potentials were generated at frequencies of ~0.6 to 1.7 Hz ( $1.09 \pm 0.05$  Hz). Addition of carbenoxolone (200  $\mu\text{M}$ ), a gap junction channel blocker, to the media stopped spontaneous activity in heterologous cell pairs. Carbenoxolone washout restored activity. Blockade of HCN2 currents by 100  $\mu\text{M}$  9-amino-1,2,3,4-tetrahydroacridine (THA) stopped spontaneous activity and subsequent washout restored it. Neither THA nor carbenoxolone affected electrically stimulated action potentials in isolated single myocytes. In summary, the inward current evoked in the genetically engineered (HCN2-expressing) cell was delivered to the cardiac myocyte via gap junctions and generated action potentials such that the cell pair could function as a pacemaker unit. This finding lays the groundwork for understanding cell-based biological pacemakers *in vivo* once an understanding of delivery and target cell geometry is defined.

(Resubmitted 19 August 2009; accepted after revision 3 September 2009; first published online 7 September 2009)

**Corresponding author** P. R. Brink: Department of Physiology and Biophysics, Stony Brook University, Stony Brook, NY 11794-8661, USA. Email: peter.brink@sunysb.edu

**Abbreviations** AP, action potential; Cx, connexin; HCN, hyperpolarization-activated cyclic nucleotide-gated; hMSCs, human mesenchymal stem cells; RFP, red fluorescent protein; SA, sinoatrial; THA, 9-amino-1,2,3,4-tetrahydroacridine.

## Introduction

Electronic pacemakers are state of the art therapies for sinus node dysfunction and high degree A–V nodal conduction block. Because of their limitations a number of biological approaches have been attempted in efforts to replace them. These include transfecting genes for  $\beta_2$  adrenergic receptors, dominant negative constructs of the molecular correlate of  $I_{K1}$  (Kir2.1) as well as native and mutant forms of members of the hyperpolarization-activated cyclic nucleotide-gated (HCN) gene family. All have been delivered by naked plasmid or adenovirus to create or enhance a biological rhythm (Edelberg *et al.* 1998; Miake *et al.* 2002; Qu

*et al.* 2003; Plotnikov *et al.* 2004, 2008; Bucchi *et al.* 2006; Tse *et al.* 2006). However, myocyte infection with adenovirus does not result in persistent expression and health concerns remain about viral vectors with more sustained action (Rosen *et al.* 2004). For these reasons, cellular approaches to create biological pacemakers have also emerged. Human mesenchymal stem cells (hMSCs), embryonic stem cells committed to a cardiac lineage, and autologous sinoatrial (SA) node myocytes have all been used (Potapova *et al.* 2004; Kehat *et al.* 2004; Zhang *et al.* 2008). While embryonic stem cell-derived cardiac myocytes and SA nodal myocytes are spontaneously active and express all the ion channels necessary to initiate and propagate an action potential, such is not the case

for hMSCs. However, when transfected with HCN genes (the molecular correlate of hyperpolarization activated pacemaker current  $I_f$ ), hMSCs can initiate a biological rhythm in the canine ventricle once they are electrically coupled (Potapova *et al.* 2004; Plotnikov *et al.* 2007).

We previously reported that a critical property of hMSCs is their formation of gap junctions with myocytes *in vitro* and *in vivo* (Potapova *et al.* 2004; Valiunas *et al.* 2004a). We now extend this work by asking three questions using an *in vitro* model: (1) What is the time course of gap junctional coupling, (2) What is the relationship between the magnitude of gap junctional conductance and transfer of HCN-induced current from transfected to non-transfected cell, and (3) Can one HCN-transfected cell induce pacemaking in an otherwise quiescent myocyte?

## Methods

### Cells and culture conditions

HeLa cells were grown in minimal essential medium supplemented with 10% fetal bovine serum (FBS), 0.1 mM non-essential amino acids, 2 mM L-glutamine, 100 U ml<sup>-1</sup> penicillin and 100 µg ml<sup>-1</sup> streptomycin (Gibco-BRL). HEK293 cells were grown in Dulbecco's modified Eagle medium (DMEM) supplemented with 10% FBS, 2 mM L-glutamine, 100 U ml<sup>-1</sup> penicillin and 100 µg ml<sup>-1</sup> streptomycin. N2A cells were grown in DMEM supplemented with 10% FBS, 0.1 mM non-essential amino acids, 2 mM L-glutamine, 100 U ml<sup>-1</sup> penicillin and 100 µg ml<sup>-1</sup> streptomycin. Human mesenchymal stem cells (hMSCs; mesenchymal stem cells, human bone marrow; Poietics™) were purchased from Clonetics/BioWhittaker (Walkersville, MD, USA) and cultured in mesenchymal stem cell (MSC) growth medium (Poietics-MSCGM; BioWhittaker).

Canine cardiac ventricular myocytes were isolated as previously described (Zygmunt, 1994; Yu *et al.* 2000). Primary cultures of the myocytes were maintained using procedures described for mouse myocytes (Zhou *et al.* 2000). Briefly, adult mongrel dogs of either sex weighing 18–22 kg were killed by intravenous injection of sodium pentobarbitone (80 mg (kg body weight)<sup>-1</sup>) and the heart removed. Canine ventricular cells were isolated using a modified Langendorf procedure by perfusing a wedge of left ventricle through a coronary artery with 0.5 mg ml<sup>-1</sup> collagenase (Type 2, Worthington, Lakewood, NJ, USA) and 0.08 mg ml<sup>-1</sup> protease (Type XVI, Sigma) for 9 to 11 min followed by tissue mincing (Zygmunt, 1994; Yu *et al.* 2000). Isolated myocytes were seeded onto laminin (Invitrogen)-coated coverslips and cultured in Medium 199 (Gibco) supplemented with 15% FBS, 2 mM L-glutamine, 100 U ml<sup>-1</sup> penicillin, 100 µg ml<sup>-1</sup> streptomycin and 50 µg ml<sup>-1</sup> gentamicin. We followed our Institutional Animal Care & Use Committee guidelines

(approved Animal Welfare Assurance Number A3011-01, approved IACUC no. 2009-0575). We used cells from 16 random-bred mongrel dogs obtained from R&R Research (Howard City, MI, USA). The experiments performed comply with the policies and regulations as specified by Drummond (2009).

A full-length mHCN2 cDNA was subcloned into the eukaryotic expression vector pIRES2-eGFP vector (Clontech Laboratories, Inc., Mountain View, CA, USA). HeLa, N2A and HEK293 cells were transiently transfected using Lipofectamine 2000 reagent (Invitrogen, Carlsbad, CA, USA) following the manufacturer's protocol. hMSCs were transfected by electroporation using the Amaxa Biosystems Nucleofector (Amaxa) technology (Hamm *et al.* 2002). Cells transfected with mHCN2/eGFP (Potapova *et al.* 2004) were co-cultured with freshly isolated canine myocytes. For purposes of identification some non-HCN2 cell populations were transfected with red fluorescent protein (RFP) (pIRES2-DsRed2, Clontech Laboratories, Inc.). Production and characterization of these cells, culture conditions and staining methods for identification of specific cells have been described previously (Valiunas *et al.* 2000, 2001, 2004b; Gemel *et al.* 2004; Potapova *et al.* 2004). Electrophysiological measurements were carried out on cells co-cultured for 1–7 days.

### Electrophysiological measurements

Experiments were carried out on heterologous cell pairs. For electrical recordings, glass coverslips with adherent cells were transferred to an experimental chamber mounted on the stage of an inverted microscope (Olympus-IX71) equipped with a fluorescence imaging system. The chamber was perfused either at room temperature (~22°C) or at ~32–35°C (for action potential recordings) with bath solution containing (in mM): NaCl, 140; MgCl<sub>2</sub>, 1; KCl, 5; CaCl<sub>2</sub>, 2; Hepes, 5 (pH 7.4); glucose, 10. In some experiments 2 mM CsCl, 2 mM BaCl<sub>2</sub> or 2 mM 4-aminopyridine (Sigma-Aldrich) were added to minimize K<sup>+</sup> currents across the cell membrane (Niggli *et al.* 1989) and to block the transient outward K<sup>+</sup> current (Castle & Slawsky, 1993). Perfusion with 200 µM of carbenoxolone (Sigma) was used to block cell–cell communication and with 100 µM of 9-amino-1,2,3,4-tetrahydroacridine (Sigma) to block HCN2-induced currents (Difrancesco *et al.* 1991). The patch pipettes were filled with solution containing (in mM): potassium aspartate, 120; NaCl, 10; MgATP, 3; Hepes, 5 (pH 7.2); EGTA, 10 (pCa ~8). Patch pipettes were pulled from glass capillaries (code GC150F-10; Harvard Apparatus) with a horizontal puller (DMZ-Universal, Zeitz-Instrumente). When filled, the resistance of the pipettes measured 2–5 MΩ. A dual whole-cell voltage-clamp method was used to control

and record the membrane potential of both cells and to measure associated membrane and junctional currents (Valiunas *et al.* 2001, 2002). The junctional currents between heterologous pairs were measured as follows. The membrane potentials of cell 1 ( $V_1$ ) and cell 2 ( $V_2$ ) were held at the same value: ( $V_1 = V_2$ ). Thereafter, the membrane potential of one of the cells was then stepped to different levels (Valiunas *et al.* 2000) to establish a trans-junctional voltage  $V_j = V_2 - V_1$ . Currents recorded from cell 2 (stepped cell) represent the sum of two components, the junctional current ( $I_j$ ) and the membrane current of cell 2; the current obtained from cell 1 corresponds to  $I_j$ . The junctional conductance  $g_j = I_j/V_j$ . A bipolar pulse protocol was used as described previously (Brink *et al.* 1997; Ramanan *et al.* 1999).

### Signal recording and analysis

Voltage and current signals were recorded using patch clamp amplifiers (Axopatch 200). The current signals were digitized with a 16 bit A/D converter (Digidata 1322A; Molecular Devices) and stored with a personal computer. Data acquisition and analysis were performed with pClamp9 software (Molecular Devices). Curve fitting and statistical analyses were performed using SigmaPlot and SigmaStat, respectively (Jandel Scientific). The results are presented as means  $\pm$  S.E.M.

## Results

### Cell-cell coupling with cardiac myocytes

We have shown previously that myocytes couple to hMSCs (Valiunas *et al.* 2004a). To better understand the nature of the heterologous coupling between hMSC and myocyte we determined the time course of coupling over a 1 week period for hMSCs and adult canine myocytes, hMSCs and neonatal rat myocytes and HeLa cells transfected with Cx43 and canine myocytes. Figure 1A and C provide examples at different time points and with different myocyte types: rat neonate and canine adult, respectively. Representative recordings of junctional currents in response to a series of transjunctional voltage steps are shown in Fig. 1B and D for the cell pairs shown in Fig. 1A and C. In the example shown in Fig. 1B both cells were clamped to the same  $V_h$ , so that  $V_1 = V_2 = 0$  mV. Starting from a  $V_h$  of 0 mV, bipolar pulses of 400 ms duration were administered to establish  $V_j$  gradients of identical amplitude with either polarity.  $V_j$  was then altered from  $\pm 10$  to  $\pm 150$  mV using increments of 20 mV. In the record shown in Fig. 1D the duration of the pulse was prolonged to 5 s, and  $V_j$  was altered from  $\pm 10$  to  $\pm 110$  mV. The data are summarized in Fig. 1E. Heterologous coupling between canine myocyte and hMSC, or HeLa cells, or hMSC and rat neonatal myocyte ranged from 1–20 nS over the 96 h interval.

Half-maximal coupling for each group occurred between 48 and 72 h.

### Expression of pacemaker (HCN2) currents

The functional expression of HCN2 in transfected hMSCs, HeLa or HEK293 cells is shown in Fig. 2 in comparison with canine ventricular myocytes which lack significant functional endogenous HCN2 currents. We previously illustrated that hMSCs possess no endogenously expressed HCN2 channels and can be stably transfected with HCN2 (Potapova *et al.* 2004). Voltage step protocols like that in Fig. 2A when applied in whole cell patch clamp on single canine ventricular myocytes display small if any  $I_f$  currents (Fig. 2B). Using the same voltage step protocol on hMSCs, HeLa and HEK293 cells transfected with HCN2 revealed robust HCN2-induced inward currents. Examples for all three transfected cell types are shown in Fig. 2C–E. Non-transfected cells did not display time-dependent currents activated by hyperpolarization (data not shown) and resembled currents shown in Fig. 2B for the non-transfected canine myocyte.

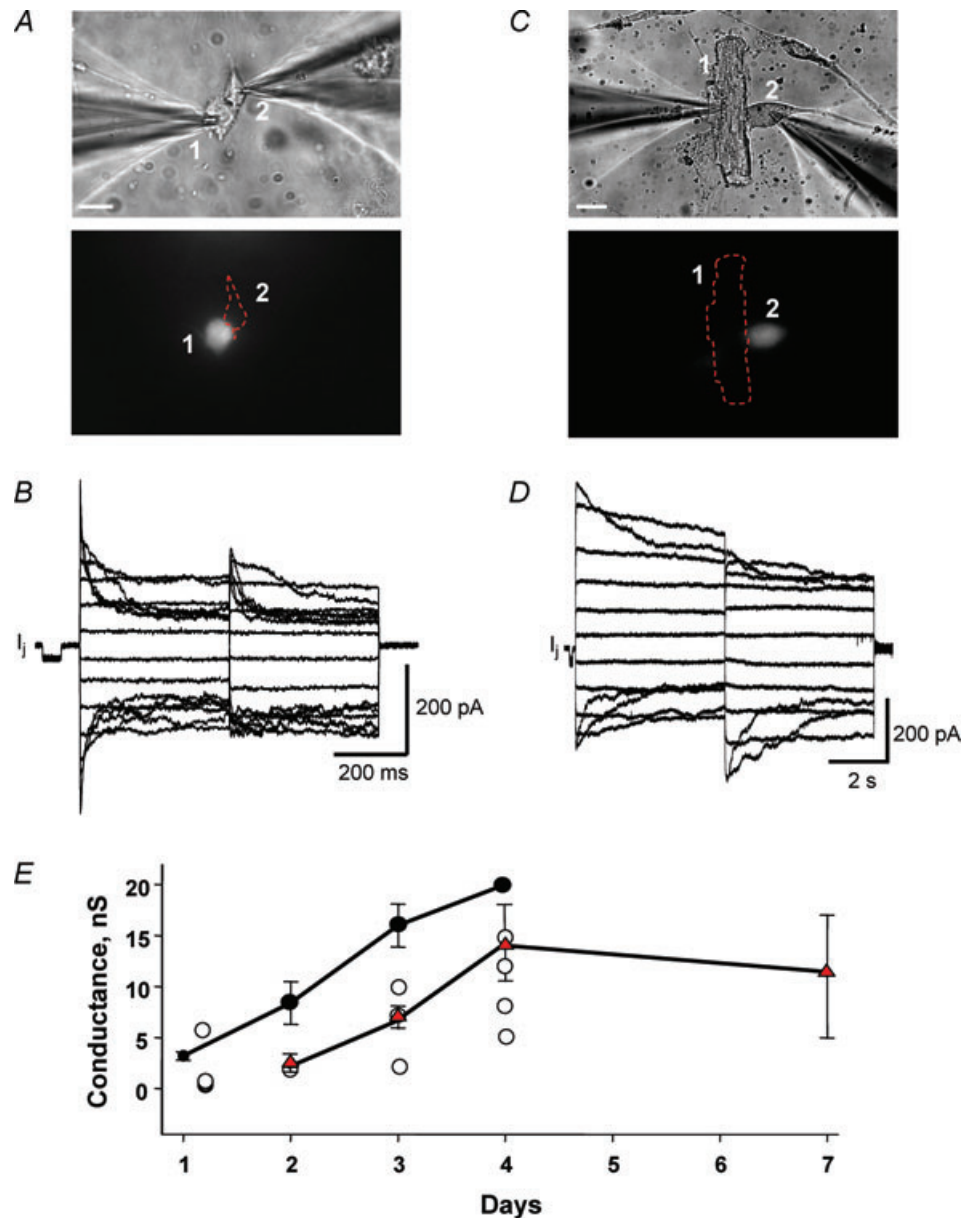
### Cell-cell transfer of pacemaker currents

Figure 3 establishes the degree of electrical coupling needed to transfer HCN2 current from the HCN2-expressing cell in a pair to the one that is non-HCN2 expressing. In Fig. 3A one cell of a pair expresses eGFP and HCN2 (green cell in the right panel) and the other expresses RFP (red cell). We routinely used this tagging method to identify and dual patch clamp cell pairs where one cell of a pair expressed HCN2 while the other did not. Figure 3B shows that no HCN2-induced current was observed in the cell not expressing HCN2, i.e. the RFP-expressing cell (middle panel) when gap junctions were not functioning (cells were not coupled yet) and no intercellular current flow was recorded (right panel). During this recording, cell 1 was held in whole cell voltage clamp (VC) mode and cell 2 was in cell attached mode. In contrast, the HCN2-expressing cell produced HCN2 currents (middle panel). When the cells in a pair were coupled, as illustrated (Fig. 3C right panel) then HCN2 currents were also observed in the RFP-expressing cell 1 (left panel) (cell 2 was in current clamp mode).

We also tested whether an HCN2 source cell can couple to a ventricular myocyte such that HCN2-induced currents are observed in both cells in the pair. Figure 4A shows a HeLa cell (cell 2) expressing Cx43, HCN2 and GFP in close apposition to a canine myocyte (cell 1). The right panel shows the fluorescent image of the HeLa cell. Both the HeLa cell and the myocyte were subsequently patch clamped. In both cells, a hyperpolarizing voltage step protocol induced robust HCN2-induced currents. Figure 4B, left panel, shows currents from the myocyte when HeLa/HCN2 cell was in current clamp mode, and

in the right panel are currents recorded from HeLa/HCN2 cell when the myocyte was held in current clamp mode. A 10 mV voltage step applied to one cell of this heterologous HeLa/HCN2–myocyte cell pair shown in Fig. 4A revealed gap junctional coupling of  $\sim 15$  nS (Fig. 4C).

The magnitude of cell to cell coupling needed to observe HCN2 currents in the recipient myocyte of a heterologous cell pair is another critical component in a gap junction-based cellular delivery system. We used different HCN2 cell sources to couple to



**Figure 1. Coupling between hMSCs and myocytes**

A, upper panel: heterologous pair of hMSC (cell 1) and neonatal rat ventricular cell (cell 2) on first day in co-culture. Lower panel: hMSC stained with cell tracker green for identification. Scale bar, 20  $\mu$ m. B, gap junction currents ( $I_j$ ) elicited from an above-shown hMSC–neonatal rat ventricle pair exhibit voltage dependence. The junctional conductance was  $\sim 3$  nS. C, upper panel: a canine ventricle cell (cell 1) and hMSC (cell 2) after 3 days in co-culture. Lower panel: eGFP fluorescence indicates expression of mHCN2 gene in the hMSC (see Methods). Scale bar, 20  $\mu$ m. D, gap junction currents recorded from the above-shown heterologous cell pair of hMSC and canine ventricular myocyte. The junctional conductance was  $\sim 9$  nS. E, summary plot of junctional conductance (mean  $\pm$  S.E.M.) versus time obtained from heterologous cell pairs of cardiac myocytes and hMSC or HeLaCx43 cells: hMSC–neonatal rat myocyte ( $\bullet$ ,  $n = 17$ ); hMSC–canine myocyte ( $\circ$ ,  $n = 12$ ); HeLaCx43–canine myocyte ( $\blacktriangle$ , red triangles  $n = 33$ ). Electrical coupling increased with time in co-culture. For hMSC–canine myocyte cell pairs individual data points are plotted with no standard error of mean plotted.

neonatal rat myocytes, canine myocytes and a cell line (N2A) to determine the relative efficiency of HCN2-induced current transfer from cell to cell. Figure 4D shows a summary graph of normalized HCN2 current (ratio of HCN2-induced currents recorded from non-transfected and HCN2-transfected cells of a pair) versus junctional conductances, illustrating that a

junctional conductance of  $\sim 15$  nS allows  $\sim 80\%$  HCN2 current transfer between cell pairs. The current transfer demonstrates that membrane impedances match for these cells. Overall in our experimental conditions, canine ventricular myocytes had an average input resistance of  $52 \pm 4$  M $\Omega$  ( $n = 15$ ) and resting potentials of  $-75 \pm 0.9$  mV ( $n = 24$ ). Coupled HCN2-transfected cells

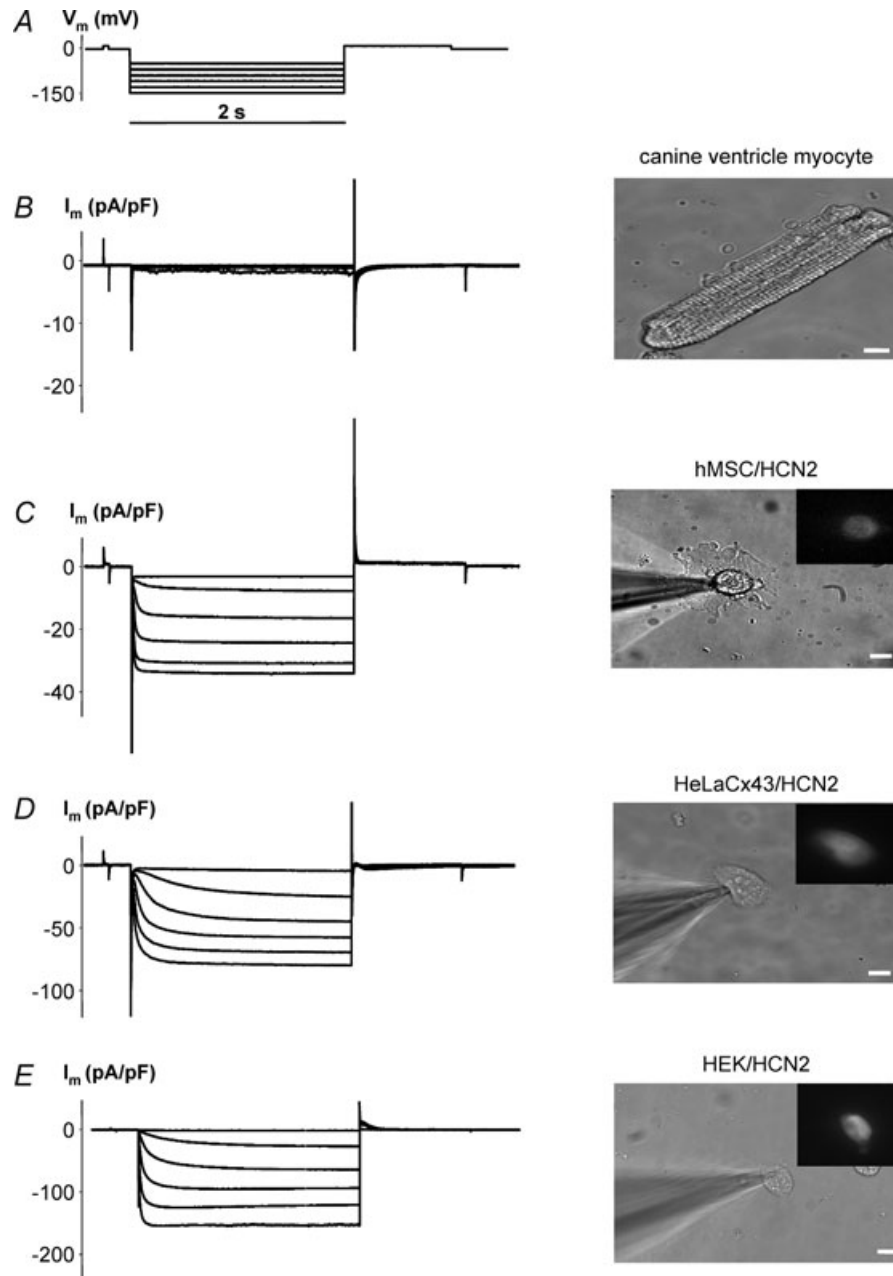


**Figure 2. Functional expression of pacemaker current in cells transfected with mHCN2 gene**

$I_m$  elicited by hyperpolarizing pulses (A) (from  $-40$  mV to  $-140$  mV) in non-transfected canine ventricle myocyte cell showed little time-dependent activation (B).  $I_m$  increased with  $V_m$ , and hyperpolarization induced voltage- and time-dependent inward currents in hMSC (C), HeLaCx43 cell (D) and HEK293 cell (E) transfected with mHCN2. Fluorescent insets indicate expression of eGFP which is expressed with mHCN2 in these cells (see Methods). 2 mM BaCl<sub>2</sub> and 2 mM 4-aminopyridine were added to the bath solution to block voltage-activated K<sup>+</sup> currents and unmask HCN2 currents. Scale bar, 10  $\mu$ m.

and myocyte pairs had resting potentials of  $-65 \pm 1.0$  mV ( $n = 37$ ).

### Pacemaker activity in a two-cell syncytium: the role of gap junctions

Figures 1–4 demonstrate that the inward current produced by HCN2 gene expression can be transferred efficiently from a source cell to a canine ventricular myocyte. We next asked whether an HCN2 source cell

coupled to a canine ventricular myocyte generates spontaneous pacing activity and if so if the appropriate channel blockers (carbenoxolone for gap junctions and 9-amino-1,2,3,4-tetrahydroacridine (THA) for HCN2) inhibit or eliminate pacing.

Figure 5A shows a single ventricular myocyte and an action potential generated by electrical stimulation via the patch electrode. Co-culturing ventricular myocytes with HeLa cells transfected with Cx43 and HCN2 produced spontaneous electrical activity in the cell pairs.

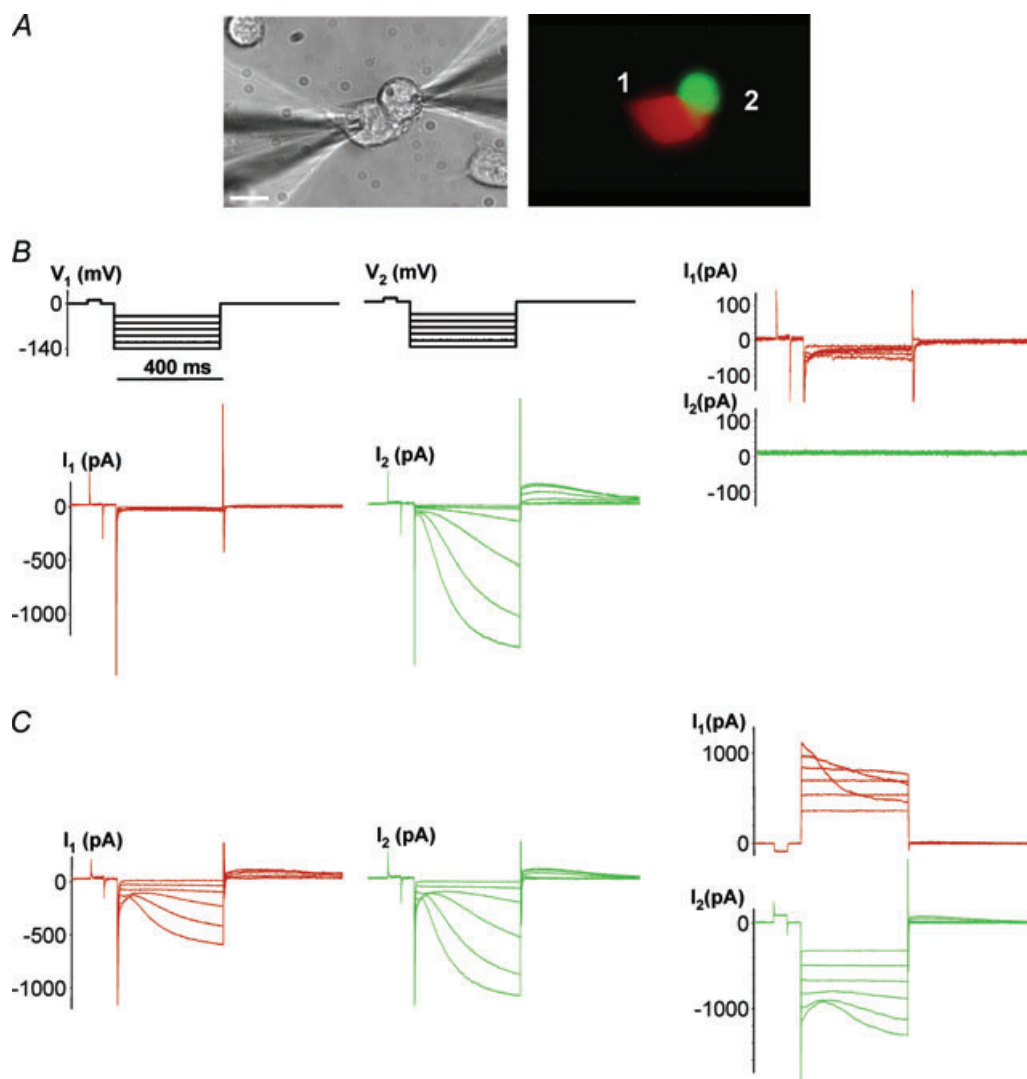


**Figure 3. Cell-cell spread of HCN2 currents**

A, N2ACx43 cell pair where one cell was transfected with mHCN2 and eGFP (green cell) and the other transfected with RFP only (red cell). Scale bar,  $10 \mu\text{m}$ . B, left panel: hyperpolarizing voltage steps did not induce HCN2 current in the red cell, but did so in the HCN2-transfected cell (middle panel) showing that there is no HCN2-induced current transfer in these uncoupled cells (cell 1, whole cell voltage clamp mode (VC); cell 2, cell attached mode). Voltage steps applied to cell 1 revealed no gap junction current ( $I_2 = 0$ ) in this cell pair, i.e.  $g_j = 0$  nS (right panel); cell 1 and cell 2, both in VC mode. C, left panel:  $I_m$  elicited by hyperpolarizing pulses in HCN2 non-transfected cell (red) showed a slow voltage- and time-dependent activation, attributable to HCN2 currents: cell 1, VC mode; cell 2, current clamp (CC) mode. Middle panel: the mHCN2-transfected cell (green) exhibited larger inward currents (cell 1, CC; cell 2, VC). Right panel: voltage steps applied to cell 2 induced voltage-gated gap junction currents ( $I_1$ ), exhibiting  $g_j$  of  $\sim 9$  nS (image not shown); cell 1 and cell 2, VC mode.

Figure 5B illustrates pacing in a cell pair incorporating a HeLaCx43/HCN2 cell coupled to a canine ventricular myocyte. The HeLa cell expressing HCN2 (cell 1) is identified based on eGFP fluorescence (right panel). The lower panel of Fig. 5B shows spontaneous action potentials (APs) recorded from the ventricular myocyte (cell 2) of the cell pair. In summary, this demonstrates that a heterologous cell pair consisting of a genetically engineered cell expressing Cx43 and HCN2 channels and a primary ventricular myocyte can function as a pacemaker

unit. If a HCN2 transfected cell is eliminated from such a two-cell pacemaker unit, the pacing function is lost (see online Supplementary Fig. 1A and Supplementary Movie 1).

Figure 6 provides a similar example when an hMSC (Fig. 6A, cell 2) is the HCN2 source and illustrates an example of an hMSC and myocyte pair working as a pacemaker unit. It further demonstrates the effects of the gap junction channel blocker carbenoxolone which reversibly inhibits pacing. Application of

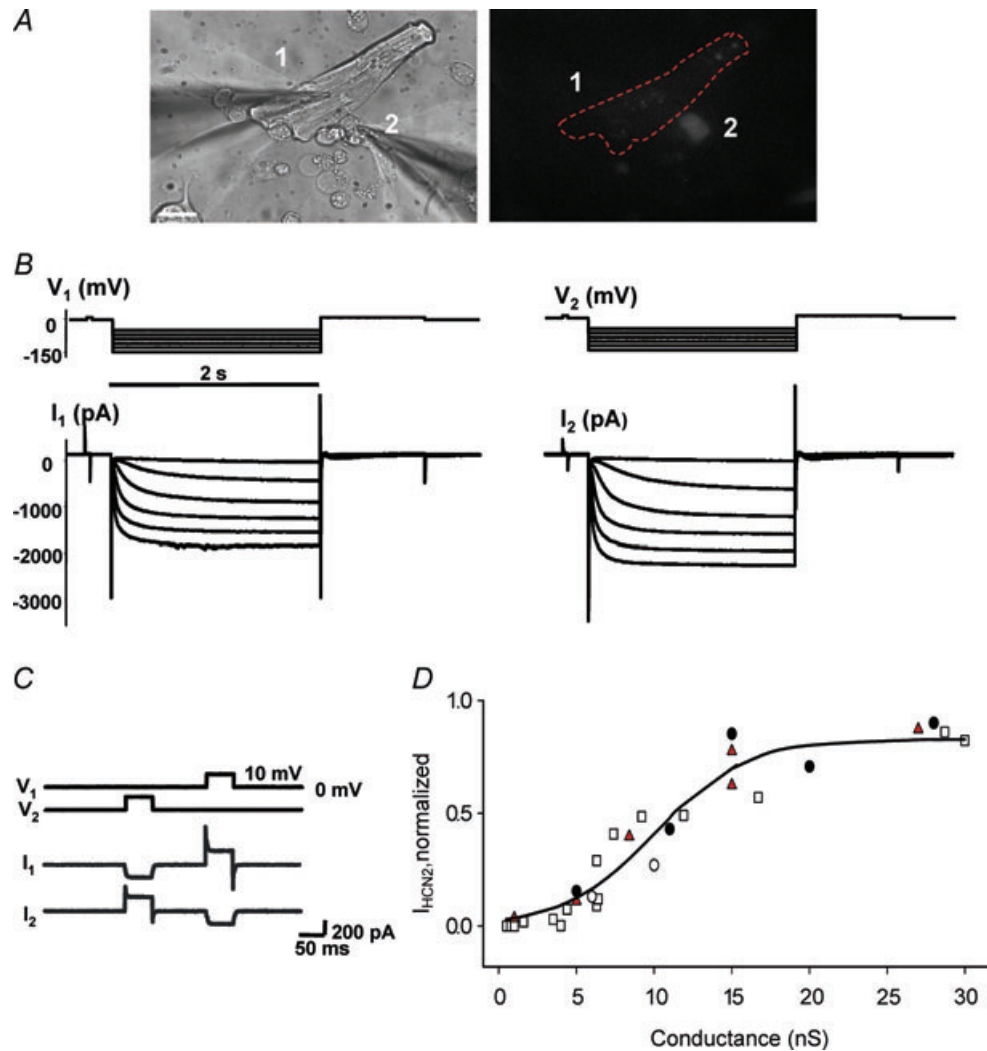


**Figure 4. HCN2 currents transfer to ventricular myocytes**

A, cell 1, canine ventricle myocyte; cell 2, HeLaCx43 cell transfected with the mHCN2 gene. Scale bar, 20  $\mu\text{m}$ . B, right panel: HCN2-induced currents recorded from mHCN2-transfected HeLaCx43 cell (cell 1, CC mode; cell 2, VC mode). Left panel: canine ventricular myocyte exhibits HCN2-induced currents (cell 1, VC mode; cell 2, CC mode). C, voltage steps (10 mV, 50 ms) applied to cell 1 and cell 2 induced currents in heterologous HeLaCx43–canine ventricular myocyte cell pair corresponding to  $g_j$  of  $\sim 15$  nS. D, relative efficiency of HCN2-induced current transfer from cell to cell. Summary plot of relative HCN2-induced current versus junctional conductance. Relative HCN2 current ratios of HCN2-induced currents recorded from pairs of non-transfected and HCN2-transfected cells: N2ACx43–N2ACx43/HCN2 ( $\square$ ), neonatal rat myocyte–N2ACx43/HCN2 ( $\bullet$ ), canine myocyte–HeLaCx43/HCN2 (red triangles) and canine myocyte–hMSCs ( $\circ$ ). Continuous line represents best fit of data to sigmoidal regression with the following parameters: maximum current,  $I_{\text{HCN2, max}} = 0.83$  and conductance at which current reaches half the maximum value,  $g_{j,0} = 10$  nS.

200  $\mu\text{M}$  carbenoxolone abolished spontaneous APs when pacemaker current flow was blocked between the hMSC and the myocyte (Fig. 6B). However, in the background of carbenoxolone, single APs were still evoked by an external electrical stimulus, S1 (right-hand side in Fig. 6B), and hyperpolarizing voltage steps applied to the stem cell (cell 2) induced HCN2 currents (Fig. 6C). Thus, we are able to record spontaneous APs which require functional gap junctions so that HCN2-induced current can be delivered to an otherwise quiescent myocyte.

To test the effect of carbenoxolone on HCN2 current a series of experiments on single HEK293 cells transfected with HCN2 were performed. Figure 6D shows a representative example where HCN2 currents from a HEK293/HCN2 cell were evoked by repetitive hyper-

polarizing voltage ( $-100$  mV, 2 s duration) pulses. HCN2-induced currents remained largely unchanged during application of carbenoxolone over 5 min. The HCN2 currents recorded from seven cells were  $1326 \pm 310$  pA and  $1064 \pm 270$  pA ( $P = 0.17$ , paired  $t$  test) before and 5 min after application of carbenoxolone, respectively. This insignificant decrease of HCN2 currents reflects the typical rundown of HCN2 currents.

In Fig. 7, the HCN2 source was a HEK293 cell transfected with HCN2. Figure 7A shows recordings of APs from a canine myocyte–HEK293/HCN2 cell pair. Spontaneous APs were abolished by superfusion with 200  $\mu\text{M}$  carbenoxolone and recovered during the followed washout (see also Supplementary Fig. 1B and Movie 2 online). Single stimulus-driven (S1) APs were

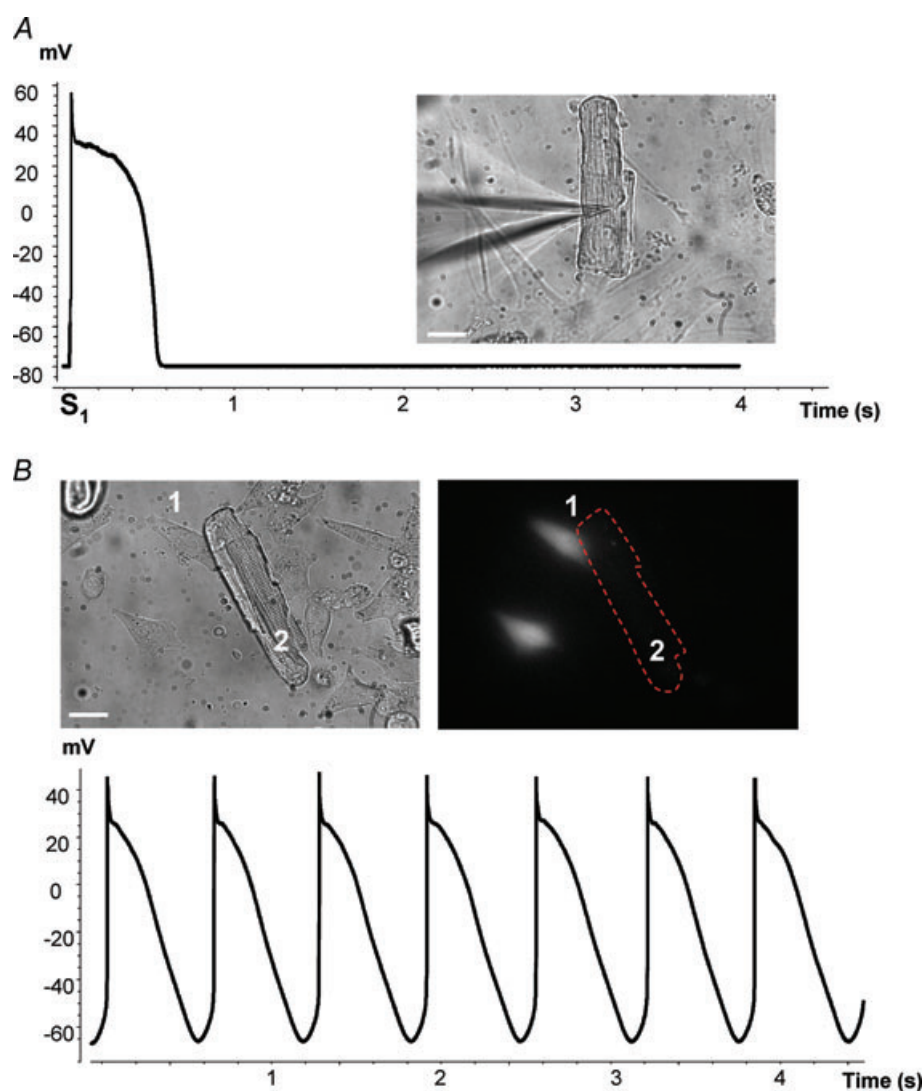


**Figure 5. Pacemaker function in cells in culture**

A, single AP derived from a canine ventricle myocyte co-cultured with non-transfected cells and excited by external stimulus (S1). B, upper panels: co-culture of canine ventricular myocytes (2) and HeLaCx43 cells (1) transfected with mHCN2 gene. Lower panel: spontaneous electrical activity of canine myocyte recorded from the above-shown co-cultured cells (3 days). Scale bar, 20  $\mu\text{m}$ .

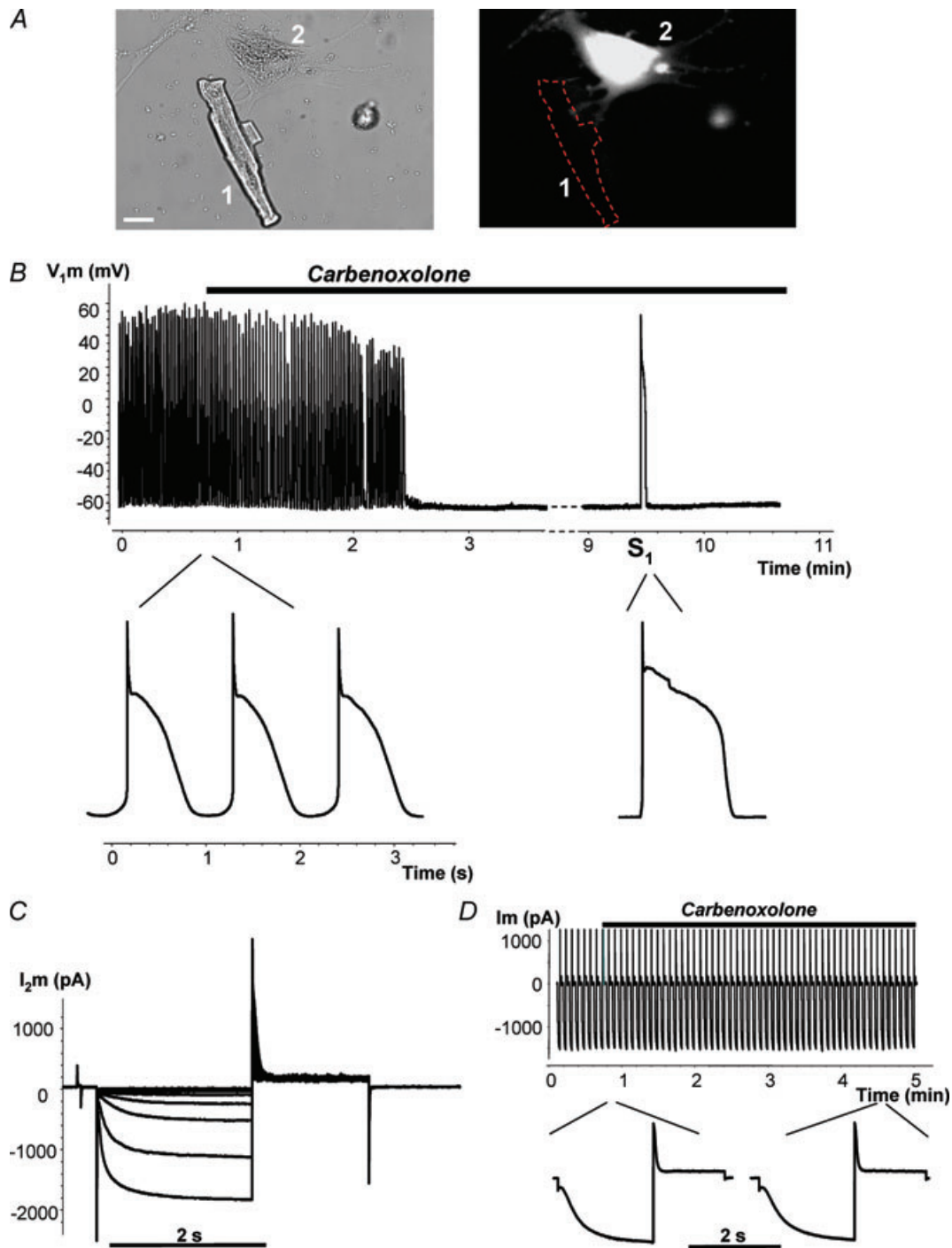


**Figure 6. Regulation of spontaneous activity by gap junction blocker carbenoxolone**

*A*, cell 1, canine ventricle myocyte; cell 2, hMSC transfected with mHCN2. Scale bar,  $20 \mu\text{m}$ . *B*, spontaneous action potential (AP) recorded from canine myocyte of the above-shown myocyte–hMSC/HCN2 cell pair. Application of  $200 \mu\text{M}$  carbenoxolone abolished spontaneous activity in a time-dependent manner. Application of an external stimulus ( $S_1$ ) evoked a single AP. Inset: APs on expanded time scale before application of carbenoxolone and during application of carbenoxolone evoked by stimulus  $S_1$ . *C*, HCN2 currents recorded from hMSC/HCN2 cell after abolishing spontaneous activity with carbenoxolone. *D*, HCN2 current recorded from HEK293/HCN2 cell, in response to hyperpolarizing voltage pulses to  $-100$  mV. Inset: segments of HCN2 current records on expanded time scale before and during application of carbenoxolone. Application of  $200 \mu\text{M}$  carbenoxolone did not affect HCN2-induced current over time (see details in text).

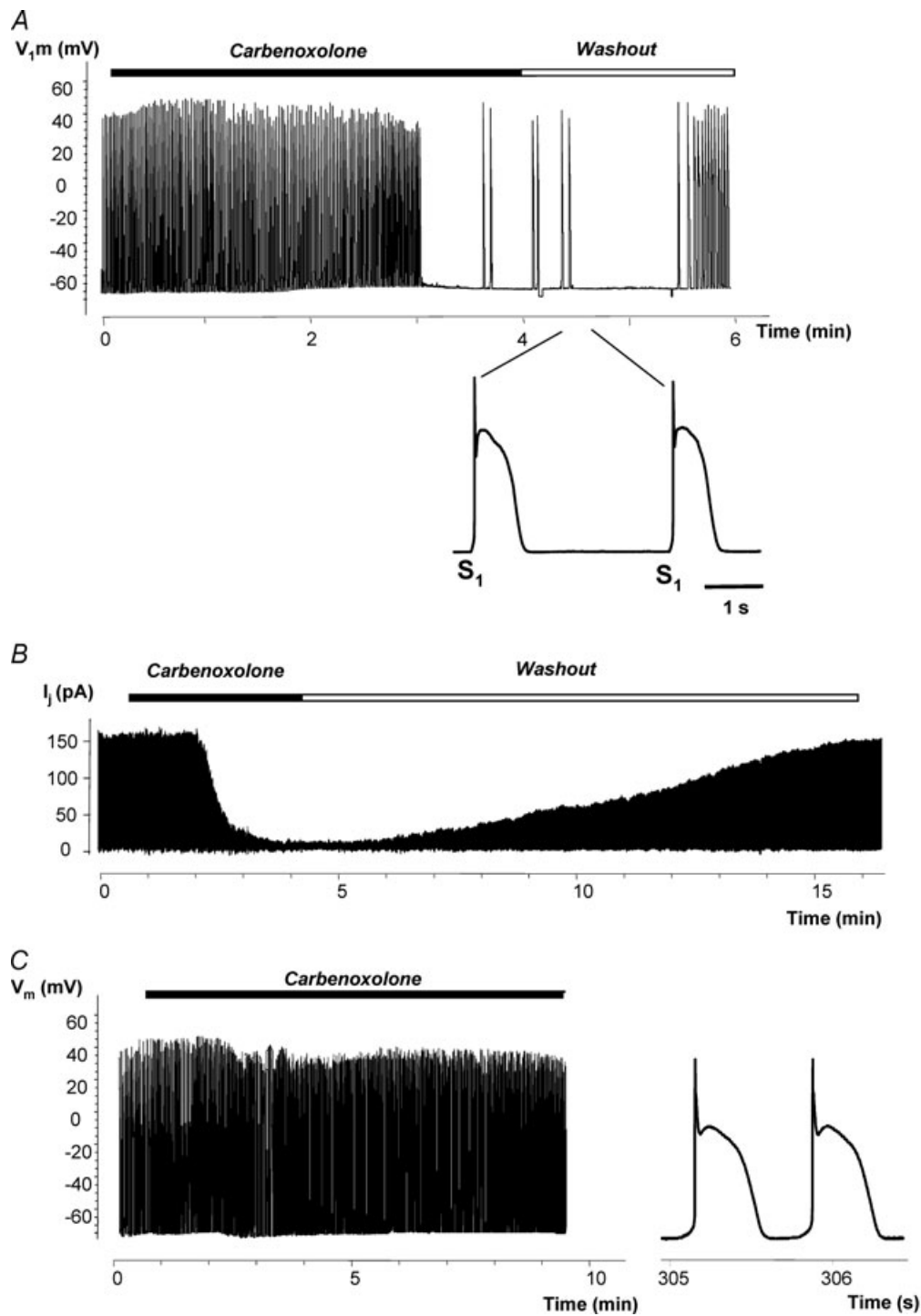


**Figure 7. Carbenoxolone and spontaneous activity**

*A*, spontaneous AP from canine myocyte–HEK293/HCN2 cell pair was abolished by perfusion with carbenoxolone and recovered during the washout that followed. Recordings were made from a canine myocyte. Inset: APs on expanded time scale evoked by extra stimulus  $S_1$  at the beginning of carbenoxolone washout. *B*, gap junction currents  $I_j$  recording from HEK293 cell pair. Application of carbenoxolone almost blocked  $I_j$  which later recovered during washout. *C*, APs recorded from single canine myocyte which exhibited spontaneous activity. Application of 200  $\mu\text{M}$  carbenoxolone did not abolish spontaneous activity. Right inset: segment of AP recording on an expanded time scale.

recorded after abolishing spontaneous activity during carbenoxolone application and early washout (inset in Fig. 7A). Figure 7B shows gap junctional currents  $I_j$  recorded from the HEK293 cell pair. Application of carbenoxolone effectively blocked gap junctional current. The cell–cell coupling recovered during washout.

Occasionally single myocytes exhibited spontaneous activity. Myocyte spontaneous activity could in part be the result of down-regulation of  $I_{K1}$ . The results presented in Supplementary Fig. 2 show that  $I_{K1}$  down-regulation occurs within the first day after cell isolation and stabilizes for the next 2–4 days (Veldkamp *et al.* 1999; Zobel *et al.* 2003). Figure 7C shows that such spontaneous activity in single myocytes is insensitive to carbenoxolone and therefore is distinguishable from HCN2-induced pacing in a two-cell pacing unit. Carbenoxolone also did not affect  $I_{K1}$  (Supplementary Fig. 2C).

Carbenoxolone blocked spontaneous activity in 20 heterologous cell pairs (myocyte–HCN2 transfected cell). In 9 of the 20 cases, washout of carbenoxolone was performed and spontaneous APs were recovered. In 6 additional cell pairs, carbenoxolone did not abolish spontaneous activity. The average

frequency of the generated AP in heterologous canine myocyte–HCN2-transfected cell pairs was  $\sim 1.1 \pm 0.05$  Hz ( $n = 32$ ; only cases with complete abolishment of AP either by carbenoxolone or THA are included). The AP frequency was indistinguishable between the various HCN2-transfected cell types.

Further proof for HCN2-induced pacing arising from an HCN2-expressing cell coupled to a myocyte is provided in Supplementary Fig. 3. A histogram of the per cent of cells contracting for days 2, 3 and 4 is shown. For each day, percentages were determined for dishes containing myocytes only, myocytes co-cultured with HEK cells and myocytes co-cultured with HCN2-expressing HEK cells. Only the last group had a significant increase in percentage of pacing units which correlates with the time course of cell-to-cell coupling.

Figure 8A shows AP frequency plotted *versus* junctional conductance from myocyte–HCN2-transfected cell pairs where junctional conductances were measured. The minimal coupling measured with induced spontaneous beating was  $\sim 2$  nS. In general, beating frequency did not show significant dependency on junctional coupling. Figure 8B illustrates AP frequency changes

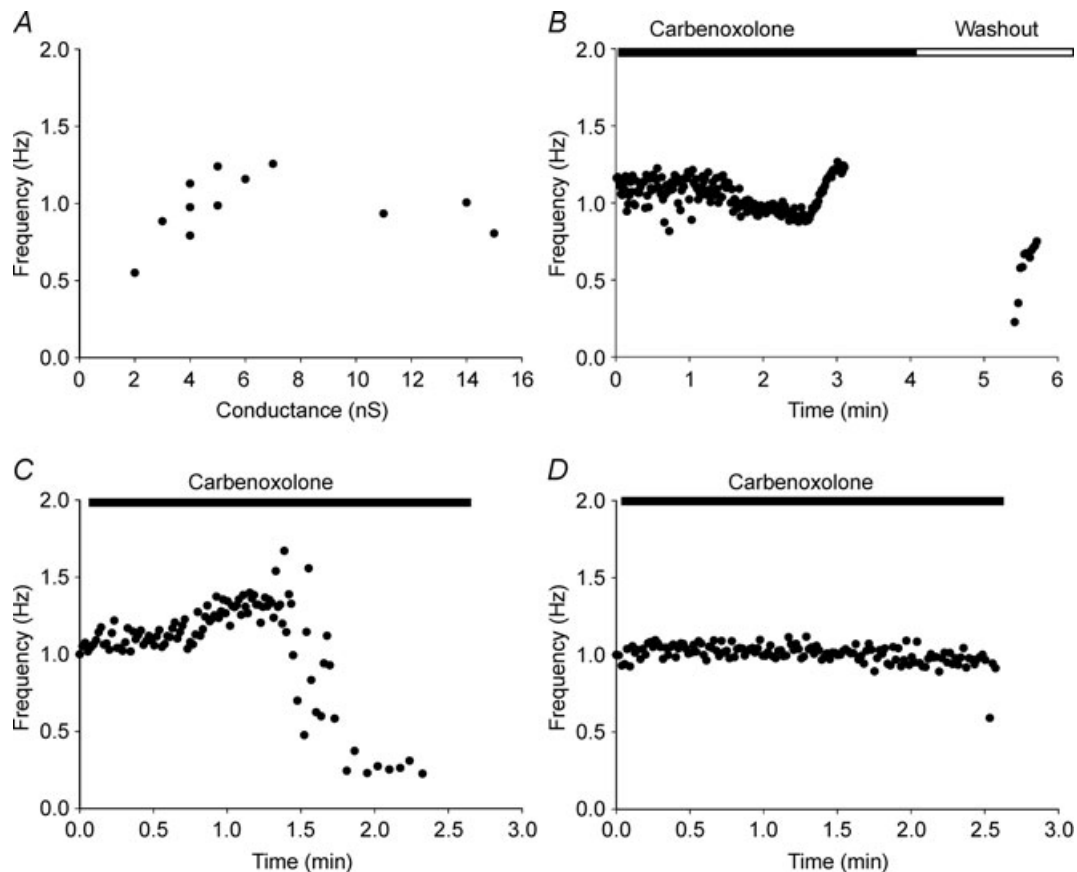


**Figure 8. Beating frequency and junctional conductance**

A, plot of spontaneous AP frequency *versus* junctional conductance in myocyte–HCN2 transfected cell pairs.

B–D, plots of AP frequency *versus* time during carbenoxolone application. See text for details.

during carbenoxolone washin and washout from an example shown in Fig. 7A. After  $\sim 1$  min of perfusion with carbenoxolone, beating frequency slightly decreased during the following 1.5 min. Later the beating frequency increased before spontaneous APs were abolished at about the 3 min time mark. During washout, i.e. recovery of gap junction conductance, the beating frequency showed a gradual increase. Stimulated APs were omitted from this example.

Although carbenoxolone blocked spontaneous APs induced by the coupled HCN2-expressing cell there were no particular patterns in frequency changes. Figure 8C and D show two more examples of AP frequency changes: slight frequency increase followed by a rapid decrease until beating stops (C) or, as in D, no frequency changes until complete AP abolishment. These data suggest that a coupling decrease/change does not significantly affect beating frequency until some critical coupling value is reached. Therefore the pacemaker unit's beating frequency rate is not limited by gap junctions despite wide changes in coupling between myocyte and the HCN2-transfected cell.

Figure 9 shows an example of the effects of 9-amino-1,2,3,4-tetrahydroacridine (THA), an  $I_f$  current blocker (Difrancesco *et al.* 1991), on spontaneous activity driven by HCN2. Figure 9A shows a heterologous pair including a canine myocyte (cell 1) and a HEK293 cell (cell 2) expressing HCN2/GFP. This pair exhibited pacing activity and Fig. 9B shows recordings of the spontaneous APs recorded from the HEK293 cell. Application of  $100 \mu\text{M}$  THA abolished spontaneous activity which returned during washout (see also Supplementary Fig. 1C and Movie 3 online). Application of an electrical stimulus (S1) evoked single APs during THA application (shaded area). Figure 9C shows HCN2 currents recorded from a HEK293/HCN2 cell. HCN2 currents gradually decreased to almost zero during application of THA. However, the gap junctional currents elicited by bipolar voltage steps (see Fig. 1C and D) in the canine myocyte–HEK293/HCN2 cell pair (Fig. 9D) was not affected by THA. Thus, the loss of pacing results from HCN2 inhibition by THA.

## Discussion

As mentioned in the Introduction, a variety of genetic and cellular approaches have successfully produced biological pacemakers in small and large mammalian hearts (Edelberg *et al.* 1998; Miake *et al.* 2002; Qu *et al.* 2003; Potapova *et al.* 2004; Kehat *et al.* 2004). If cells are to be employed there are two questions that must be answered. First, do the cells have the necessary complement of native ion channels to both initiate and conduct an action potential? Second, how can these delivery cells be integrated into the native cardiac

syncytium? The answer to the first question depends on the stem cell type. Human embryonic stem cells, and autologous sinus node myocytes, express the necessary proteins to both initiate pacemaker activity and conduct the cardiac impulse (Kehat *et al.* 2002; He *et al.* 2003; Sartiani *et al.* 2007; Zhang *et al.* 2008). Human mesenchymal stem cells do not natively express the channels for either function but can be transfected with HCN genes to provide a pacemaker current. As to the second question, there are two ways to introduce cells into the syncytium, either by gap junctions (Valiunas *et al.* 2004a; Potapova *et al.* 2004) or by membrane fusion (Cho *et al.* 2007). Membrane fusion is induced by an agent (polyethylene-glycol) which may have toxic side effects, and the long-term effects of this fusion on cell properties is unknown. In the current study, we have investigated gap junctional coupling as a means to induce pacemaker activity.

We have tested the hypothesis that an HCN2-expressing non-myocyte cell coupled by gap junction channels to a canine ventricular myocyte could drive spontaneous activity in the ventricular myocyte, effectively creating a two-cell pacemaker syncytium. The endogenous expression of an HCN gene in sinus node myocytes generates the inward current necessary for cardiac excitation. In this study, we used cell types endogenously expressing or stably transfected with Cx43 and transfected with HCN2 and expressing mHCN2-induced current. These HCN2-transfected cells, unlike SA node cells, are not excitable because of the lack of the complement of channels required for action potential generation. However, these cells can serve as HCN donors, generating depolarizing current which spreads to coupled myocytes, inducing spontaneous activity in otherwise quiescent ventricular myocytes. Supplementary Fig. 4 further demonstrates that HCN2 currents were periodically activated in transfected cells during AP waveform stimulation. Our data show that as long as the non-myocyte cells express the pacemaker current and couple to cardiac myocytes via gap junctions, they will function as a pacemaker unit in a fashion analogous to the normal sinoatrial node pacemaker.

Previous studies have provided evidence in support of this hypothesis. The first requirement is adequate expression of connexins. The non-myocytic hMSCs and HEK293 cells both express connexins, the former, Cx43 and Cx40, the latter Cx43. In addition, these cell types form functional channels with other homologous cells (Valiunas *et al.* 2001, 2002, 2004a; Gemel *et al.* 2004). HeLa cells do not normally express connexins but for the studies shown here we use a HeLa cell line that stably expresses Cx43 (Valiunas *et al.* 2002).

A second requirement is heterologous coupling of non-myocyte to myocyte. HMSCs couple heterologously to myocytes *in vitro* (Valiunas *et al.* 2004a) and to ventricular myocytes *in vivo* (Potapova *et al.* 2004).

Further, our steady-state  $I-V$  curves for all three cell types have revealed single whole cell resistances of 1 G $\Omega$  and above, and resting potentials between  $-40$  and  $-60$  mV. These values are compatible with data for these cell types published by others (Niemeyer *et al.* 2001; Potapova

*et al.* 2004; Spletstoeser *et al.* 2007; Tao *et al.* 2007). The whole cell resistance values are large enough to eliminate these cells as significant sinks once coupled to a ventricular myocyte which has an input resistance of  $\sim 25$  M $\Omega$  to 50 M $\Omega$  (when calculated from reported

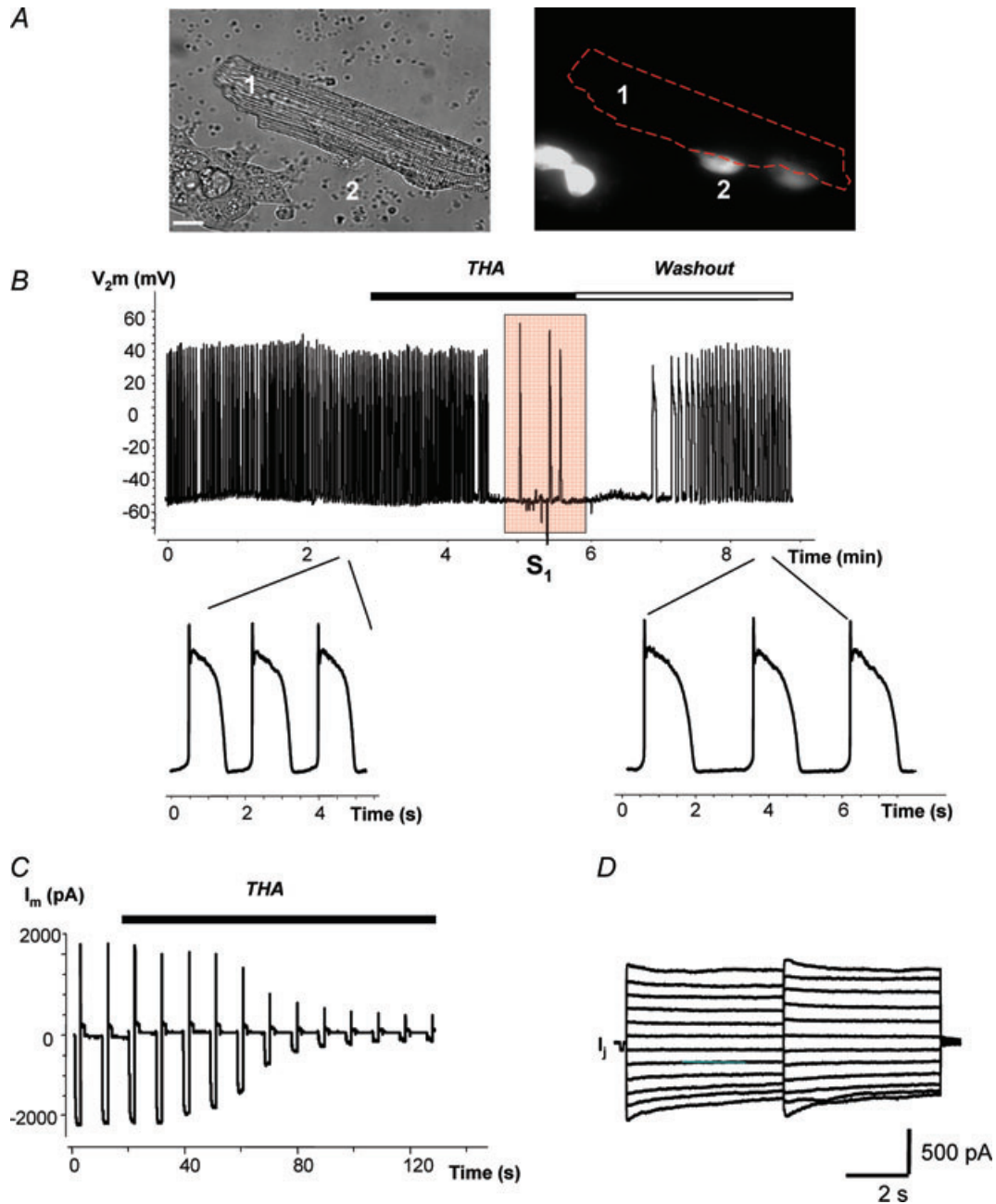


**Figure 9. Regulation of spontaneous activity by 9-amino-1,2,3,4-tetrahydroacridine (THA)**

A, cell 1, canine ventricular myocyte; cell 2, HEK293 cell transfected with mHCN2. Scale bar, 10  $\mu$ m. B, spontaneous action potential (AP) recorded from the HEK293 cell of the myocyte–HEK293/HCN2 cell pair shown in A. Application of 100  $\mu$ M THA abolished spontaneous activity which was recovered during washout. Application of an extra stimulus (S1) evoked single APs during THA application (shaded area). Inset: APs on expanded time scale before application of THA and after washout from THA. C, HCN2 current recorded from HEK293/HCN2 cell, in response to hyperpolarizing voltage pulses to  $-100$  mV. Application of 100  $\mu$ M THA blocked the HCN2-induced current in a time-dependent manner, but did not block gap junction current  $I_j$  recorded from canine myocyte–HEK293/HCN2 cell pair (D).

specific membrane resistance; Daut, 1982; Sakmann & Trube, 1984). These values are in good agreement with input resistance values of 52 M $\Omega$  measured from canine ventricular myocytes in our experiments.

Our experimental protocols demonstrated that a canine ventricular myocyte and an HCN2-expressing cell can function as a pacing unit over a wide range of cell–cell coupling. This conclusion is based on two types of data both shown in Fig. 8. First, there is no correlation between pacing frequency and magnitude of gap junctional coupling in spontaneously active cell pairs. Second, application of a gap junctional uncoupler carbenoxolone did not consistently affect spontaneous pacing rate until very low values of cell–cell (<2–3 nS) coupling were achieved. This is a surprising result. Possibly it reflects two opposing effects of uncoupling: (1) a reduced level of HCN2-induced current transfer to the pacing cell which should slow pacing rate, and (2) an increase in inward current due to hyperpolarization of the myocyte. This hyperpolarization should increase sodium channel availability particularly in the depolarized voltage range studied here (–65 mV for coupled myocytes and –75 mV for single myocytes) and hyperpolarize the threshold potential enhancing spontaneous rate. Other inward currents like  $I_{Na/Ca}$  could contribute as could the inward current induced by a significant transjunctional voltage between the more depolarized HEK cell and the hyperpolarized myocyte. Alternatively, there may be an intrinsic pacemaker frequency of the cell pair determined largely by the kinetics of HCN2 and the membrane resistance of the myocyte. Detailed computer simulations will be required to answer this question in a manner similar to the theoretical studies executed by Joyner *et al.* (1998) examining coupling of an SA node myocyte to an atrial myocyte.

In this study we have demonstrated that the critical electrical cell–cell coupling between cardiac myocytes and mHCN2-transfected cells is obtained within 24 to 36 h, allowing the cell pair to function as a pacemaker unit. Our data provide clear evidence of the essential role of gap junction channels composed of Cx43 and possibly Cx40 in the transfer of HCN2-induced currents from source cell to myocyte. For any cell expressing HCN2 and a connexin able to form homotypic, heteromeric or heterotypic channels with Cx43, a two-cell functional syncytium with a ventricular myocyte is predicted to be possible.

In summary, if cells are to be used as a delivery system for electrical regeneration of cardiac function, then an understanding of their means of integration into the cardiac syncytium is essential. In this study we have demonstrated in our *in vitro* system that a quiescent adult canine ventricular myocyte can be induced to pace by coupling it to a cell overexpressing the HCN2 gene. This is the first step towards understanding the

basis of *in vivo* biological pacemakers created by delivery of HCN2-transfected hMSCs to the canine ventricle. Further understanding will require a quantitative picture of the delivery and target cell geometries *in vivo*. It will also require computations employing the slightly larger  $I_{K1}$  existing in the myocytes prior to cell culture. The present study unambiguously demonstrates the viability of cell-based delivery of pacemaker currents.

## References

- Brink PR, Cronin K, Banach K, Peterson E, Westphale EM, Seul KH, Ramanan SV & Beyer EC (1997). Evidence for heteromeric gap junction channels formed from rat connexin43 and human connexin37. *Am J Physiol Cell Physiol* **273**, C1386–C1396.
- Bucchi A, Plotnikov AN, Shlapakova I, Danilo P, Kryukova Y, Qu JH *et al.* (2006). Wild-type and mutant HCN channels in a tandem biological-electronic cardiac pacemaker. *Circulation* **114**, 992–999.
- Castle NA & Slawsky MT (1993). Characterization of 4-aminopyridine block of the transient outward  $K^+$  current in adult rat ventricular myocytes. *J Pharmacol Exp Ther* **265**, 1450–1459.
- Cho HC, Kashiwakura Y & Marban E (2007). Creation of a biological pacemaker by cell fusion. *Circ Res* **100**, 1112–1115.
- Daut J (1982). The passive electrical properties of guinea-pig ventricular muscle as examined with a voltage-clamp technique. *J Physiol* **330**, 221–242.
- Difrancesco D, Porciatti F, Janigro D, Maccaferri G, Mangoni M, Tritella T, Chang F & Cohen IS (1991). Block of the cardiac-pacemaker current ( $I_f$ ) in the rabbit sinoatrial node and in canine Purkinje-fibres by 9-amino-1,2,3,4-tetrahydroacridine. *Pflugers Arch* **417**, 611–615.
- Drummond GB (2009). Reporting ethical matters in *The Journal of Physiology*: standards and advice. *J Physiol* **587**, 713–719.
- Edelberg JM, Aird WC & Rosenberg RD (1998). Enhancement of murine cardiac chronotropy by the molecular transfer of the human  $\beta_2$  adrenergic receptor cDNA. *J Clin Invest* **101**, 337–343.
- Gemel J, Valiunas V, Brink PR & Beyer EC (2004). Connexin43 and connexin26 form gap junctions, but not heteromeric channels in co-expressing cells. *J Cell Sci* **117**, 2469–2480.
- Hamm A, Krott N, Breibach I, Blindt R & Bosserhoff AK (2002). Efficient transfection method for primary cells. *Tissue Eng* **8**, 235–245.
- He JQ, Ma Y, Lee Y, Thomson JA & Kamp TJ (2003). Human embryonic stem cells develop into multiple types of cardiac myocytes: action potential characterization. *Circ Res* **93**, 32–39.
- Joyner RW, Kumar R, Golod DA, Wilders R, Jongsma HJ, Verheijck EE, Bouman L, Goolsby WN & Van Ginneken AC (1998). Electrical interactions between a rabbit atrial cell and a nodal cell model. *Am J Physiol* **274**, H2152–H2162.

- Kehat I, Gepstein A, Spira A, Itskovitz-Eldor J & Gepstein L (2002). High-resolution electrophysiological assessment of human embryonic stem cell-derived cardiomyocytes: a novel in vitro model for the study of conduction. *Circ Res* **91**, 659–661.
- Kehat I, Khimovich L, Caspi O, Gepstein A, Shofti R, Arbel G *et al.* (2004). Electromechanical integration of cardiomyocytes derived from human embryonic stem cells. *Nat Biotechnol* **22**, 1282–1289.
- Miake J, Marban E & Nuss HB (2002). Gene therapy – biological pacemaker created by gene transfer. *Nature* **419**, 132–133.
- Niemeyer MI, Cid LP, Barros LF & Sepulveda FV (2001). Modulation of the two-pore domain acid-sensitive K<sup>+</sup> channel TASK-2 (KCNK5) by changes in cell volume. *J Biol Chem* **276**, 43166–43174.
- Niggli E, Rudisuli A, Maurer P & Weingart R (1989). Effects of general anaesthetics on current flow across membranes in guinea pig myocytes. *Am J Physiol Cell Physiol* **256**, C273–C281.
- Plotnikov AN, Bucchi A, Shlapakova I, Danflo P, Brink PR, Robinson RB, Cohen IS & Rosen MR (2008). HCN212-channel biological pacemakers manifesting ventricular tachyarrhythmias are responsive to treatment with I<sub>f</sub> blockade. *Heart Rhythm* **5**, 282–288.
- Plotnikov AN, Shlapakova I, Szabolcs MJ, Danilo P, Lorell BH, Potapova IA *et al.* (2007). Xenografted adult human mesenchymal stem cells provide a platform for sustained biological pacemaker function in canine heart. *Circulation* **116**, 706–713.
- Plotnikov AN, Sosunov EA, Qu JH, Shlapakova IN, Anyukhovskiy EP, Liu LL *et al.* (2004). Biological pacemaker implanted in canine left bundle branch provides ventricular escape rhythms that have physiologically acceptable rates. *Circulation* **109**, 506–512.
- Potapova I, Plotnikov A, Lu Z, Danilo P Jr, Valiunas V, Qu J *et al.* (2004). Human mesenchymal stem cells as a gene delivery system to create cardiac pacemakers. *Circ Res* **94**, 952–959.
- Qu JH, Plotnikov AN, Danilo P, Shlapakova I, Cohen IS, Robinson RB & Rosen MR (2003). Expression and function of a biological pacemaker in canine heart. *Circulation* **107**, 1106–1109.
- Ramanan SV, Brink PR, Varadaraj K, Peterson E, Schirrmacher K & Banach K (1999). A three-state model for connexin37 gating kinetics. *Biophys J* **76**, 2520–2529.
- Rosen MR, Brink PR, Cohen IS & Robinson RB (2004). Genes, stem cells and biological pacemakers. *Cardiovas Res* **64**, 12–23.
- Sakmann B & Trube G (1984). Conductance properties of single inwardly rectifying potassium channels in ventricular cells from guinea-pig heart. *J Physiol* **347**, 641–657.
- Sartiani L, Bettiol E, Stillitano F, Mugelli A, Cerbai E & Jaconi ME (2007). Developmental changes in cardiomyocytes differentiated from human embryonic stem cells: a molecular and electrophysiological approach. *Stem Cells* **25**, 1136–1144.
- Spletstoesser F, Florea AM & Busselberg D (2007). IP3 receptor antagonist, 2-APB, attenuates cisplatin induced Ca<sup>2+</sup>-influx in HeLa-S3 cells and prevents activation of calpain and induction of apoptosis. *Br J Pharmacol* **151**, 1176–1186.
- Tao R, Lau CP, Tse HF & Li GR (2007). Functional ion channels in mouse bone marrow mesenchymal stem cells. *Am J Physiol Cell Physiol* **293**, C1561–C1567.
- Tse HF, Xue T, Lau CP, Siu CW, Wang K, Zhang QY *et al.* (2006). Bioartificial sinus node constructed via *in vivo* gene transfer of an engineered pacemaker HCN channel reduces the dependence on electronic pacemaker in a sick-sinus syndrome model. *Circulation* **114**, 1000–1011.
- Valiunas V, Beyer EC & Brink PR (2002). Cardiac gap junction channels show quantitative differences in selectivity. *Circ Res* **91**, 104–111.
- Valiunas V, Doronin S, Valiuniene L, Potapova I, Zuckerman J, Walcott B *et al.* (2004a). Human mesenchymal stem cells make cardiac connexins and form functional gap junctions. *J Physiol* **555**, 617–626.
- Valiunas V, Gemel J, Brink PR & Beyer EC (2001). Gap junction channels formed by coexpressed connexin40 and connexin43. *Am J Physiol Heart Circ Physiol* **281**, H1675–H1689.
- Valiunas V, Mui R, McLachlan E, Valdimarsson G, Brink PR & White TW (2004b). Biophysical characterization of zebrafish connexin35 hemichannels. *Am J Physiol Cell Physiol* **287**, C1596–C1604.
- Valiunas V, Weingart R & Brink PR (2000). Formation of heterotypic gap junction channels by connexins 40 and 43. *Circ Res* **86**, E42–E49.
- Veldkamp MW, de Jonge B & Van Ginneken AC (1999). Decreased inward rectifier current in adult rabbit ventricular myocytes maintained in primary culture: a single-channel study. *Cardiovasc Res* **42**, 424–433.
- Yu H, Gao J, Wang H, Wymore R, Steinberg S, McKinnon D, Rosen MR & Cohen IS (2000). Effects of the renin-angiotensin system on the current I<sub>to</sub> in epicardial and endocardial ventricular myocytes from the canine heart. *Circ Res* **86**, 1062–1068.
- Zhang H, Shlapakova IN, Zhao X, Danilo P, Robinson RB, Qu D, Huang S, Zhang B, Xu Z, Rosen MR & Lau DH (2008). Biological pacing by implantation of autologous sinoatrial node cells into the canine right ventricle. *Circulation* **118**, S427–S428.
- Zhou YY, Wang SQ, Zhu WZ, Chruscinski A, Kobilka BK, Ziman B *et al.* (2000). Culture and adenoviral infection of adult mouse cardiac myocytes: methods for cellular genetic physiology. *Am J Physiol Heart Circ Physiol* **279**, H429–H436.
- Zobel C, Cho HC, Nguyen TT, Pekhletski R, Diaz RJ, Wilson GJ & Backx PH (2003). Molecular dissection of the inward rectifier potassium current (I<sub>K1</sub>) in rabbit cardiomyocytes: evidence for heteromeric co-assembly of K<sub>ir2.1</sub> and K<sub>ir2.2</sub>. *J Physiol* **550**, 365–372.
- Zygmunt AC (1994). Intracellular calcium activates a chloride current in canine ventricular myocytes. *Am J Physiol Heart Circ Physiol* **36**, H1984–H1995.

### Author contributions

V.V. designed and executed the majority of experiments, performed analysis and interpretation of data, wrote and edited the manuscript. G.K. designed and conducted specific double

and single patch clamp experiments, performed analysis and interpretation of data. L.V. and C.G. maintained tissue cultures, helped to design specific experiments and provided text for portions of the Methods section. H.Z.W. and L.L. conducted specific single patch clamp experiments and performed data analysis. R.B.R. edited the manuscript and provided critical analysis of the data. M.R.R. provided key insights for experimental design and edited the manuscript. I.S.C. was involved in experimental design, data interpretation and edited the manuscript. P.R.B. oversaw experimental design, data

analysis and interpretation, wrote and edited the manuscript. All parts of this study were conducted at the Department of Physiology and Biophysics, Stony Brook University.

### **Acknowledgements**

This work was supported by grants: American Heart Association (AHA) 0335236N (to V.V.), HL28958, Boston Scientific and NYSTEM institutional support.